18th Annual International Conference of the IEEE Engineering in Medicine and Biology Society, Amsterdam 1996
3.5.2: EEG/MEG - Inverse Problem and Mapping

DYNAMIC BAYESIAN IMAGING USING THE MAGNETOENCEPHALOGRAM[1]

†J. W. Phillips, †R. M. Leahy, and ‡J. C. Mosher
†Univ. of Southern California, Los Angeles, CA, 90089-2564(jamesphi@sipi.usc.edu, leahy@sipi.usc.edu)
‡Los Alamos National. Laboratory, Los Alamos, New Mexico, 87545 (mosher@lanl.gov)

Abstract - We describe a new approach to imaging neuronal current sources from magnetoencephalogram (MEG) measurements associated with sensory, motor or cognitive brain activation. Previous approaches use weighted minimum norm inverse methods which produce spatially smooth solutions. These results are inconsistent with functional activation studies using fMRI or PET, which reveal a sparse localized nature of activation in the cerebral cortex. We use a Bayesian technique with a Gibbs prior reflecting this expectation. The prior, combined with a Gaussian likelihood function, forms the posterior density, which we can maximize to produce a non-linear estimate of the primary neural current field. We also investigate marginalizing out the amplitude time-series, and compare the joint and marginal MAP estimates. We apply the methods to phantom data and show favorable performance in comparison to minimum norm approaches.

I. Minimum Norm Approach to MEG Imaging

An array of biomagnetometers may be used to measure the spatio-temporal magnetoencephalogram (MEG) produced by the brain. We wish to construct an image of the neural activity that produced the magnetic field. This inverse problem is highly ill-posed due to the ambiguities inherent in determining the current distribution within an object from measurements of the external magnetic field and by the limited number of sensor measurements available.

Physiological models for the MEG assume primary sources are constrained to the cortex with flow oriented normal to the local surface. By tesselating the cortex with N disjoint regions and representing the sources in each region by an equivalent constrained dipole with amplitude time-series $y_i(t), t = 1 \ldots L$, the problem can be expressed in terms of a linear model. We may relate the time series $\mathbf{y}$ (NxL) and the M MEG measurements $\mathbf{b}$ (MxL) as $\mathbf{b} = \mathbf{G}\mathbf{y} + \mathbf{n}$, where the i'th row of the MxN system matrix $\mathbf{G}$ is a discrete representation of the lead field (sensitivity) of the i'th sensor. The j'th column of $\mathbf{G}$ specifies the gain vector for the j'th constrained dipole component. The MxL matrix $\mathbf{n}$ represents noise generated within the sensor and by unwanted electromagnetic sources.

Due to the ill-posedness of the inverse problem, imaging methods are concerned with finding a way to choose within a set of images that produce essentially the same fit to the data. Weighted minimum l_2-norm approaches to the linear inverse problem solve the constrained optimization problem:

$$\mathbf{y}_{wmn} = \arg\min_{\mathbf{y}} \; \mathbf{y}^T \mathbf{C}_y^{-1} \mathbf{y} \quad \text{such that} \quad |\mathbf{b} - \mathbf{G}\mathbf{y}|^2 = 0 \qquad (1)$$

[1]This work supported by the National Institute of Mental Health, Grant No. R01-MH53213.

where $\mathbf{C}_y$ is an arbitrary symmetric positive definite matrix. Writing $\mathbf{C}_y = \mathbf{W}\mathbf{W}^T$, we can form the solution as,

$$\mathbf{y}_{wmn} = \mathbf{W}\mathbf{W}^T\mathbf{G}^T(\mathbf{G}\mathbf{W}\mathbf{W}^T\mathbf{G}^T)^{-1}\mathbf{b}. \qquad (2)$$

Several forms of $\mathbf{W}$ have been proposed for MEG imaging applications. In the normalized minimum norm method [1], $\mathbf{W}_{norm} = \mathrm{diag}(1/\|\mathbf{g}_1\|, 1/\|\mathbf{g}_2\| \ldots, 1/\|\mathbf{g}_N\|)$ where $\|\mathbf{g}_i\|$ is the Euclidean norm of the i'th column of $\mathbf{G}$. This weighting is designed to compensate for the reduced sensitivity of MEG to deep sources. The LORETA technique [2] uses a weighting matrix $\mathbf{W}_L = \mathbf{W}_{norm}\mathbf{B}^{-1}$. The Laplacian operator $\mathbf{B}$ tends to smooth the reconstruction.

II. A New Bayesian Approach

Functional activation studies using fMRI and PET show the primary sources of MEG to be sparse and focal, so we use this information in reconstructing the image. We use a Bayesian paradigm in which the source is modeled as a random process. Since we assume sparse sources, most will be zero amplitude. To facilitate this, we use a Nx1 binary indicator process $\mathbf{x}$ to model whether each source dipole is *on* (x_i =1) or *off* (x_i =0). Those sites that are active are assumed to have a temporally white Gaussian amplitude time series. We write $\mathbf{y} = \mathbf{X}\mathbf{z}$, where $\mathbf{X} = \mathrm{diag}(\mathbf{x})$ and the NxL amplitude process $\mathbf{z}$ is defined where $\mathbf{z}_{ij}$ is the amplitude of source i at time j. Assuming independence of the indicator and amplitude processes, we can write the posterior probability as,

$$p(\mathbf{x}, \mathbf{z}|\mathbf{b}) = \frac{p(\mathbf{b}|\mathbf{x}, \mathbf{z})p(\mathbf{x})p(\mathbf{z})}{p(\mathbf{b})}. \qquad (3)$$

We use a Markov Random Field for the prior on $\mathbf{x}$ where sparse focal sources have a higher occurrence probability than more distributed sources. We define $p(\mathbf{x})$ to be a Gibbs distribution with energy function,

$$V(\mathbf{x}) = \sum_i \left[\underbrace{\alpha_i x_i}_{\text{Sparseness Term}} + \underbrace{\beta_i \Big[\sum_{j \in \xi_i} (x_i - x_j)^2 \Big]^Q}_{\text{Clustering Term}} \right] \qquad (4)$$

where $\alpha_i > 0$ and $\beta_i > 0$ determine the relative weights of the sparseness and clustering terms, and Q determines the clustering strength defined over each pixel's neighbors ξ_i. Note, since $\mathbf{x}$ is constant for the entire time series, we have effectively built a temporal correlation into the prior.

We define $\mathbf{z}$ to be a temporally white Gaussian process with zero mean and covariance $\mathbf{C}_z$. Using the priors on $\mathbf{x}$ and $\mathbf{z}$ and assuming the noise process $\mathbf{n}$ is zero mean Gaussian with covariance $\mathbf{C}_n$, we can form the posterior probability as a Gibbs distribution with an energy function given by,

$$U(\mathbf{x}, \mathbf{z}|\mathbf{b}) = \tfrac{1}{2}\mathrm{Tr}\{(\mathbf{b}-\mathbf{G}\mathbf{X}\mathbf{z})^T\mathbf{C}_n^{-1}(\mathbf{b}-\mathbf{G}\mathbf{X}\mathbf{z}) + \mathbf{z}^T\mathbf{C}_z^{-1}\mathbf{z}\} + V(\mathbf{x}). \qquad (5)$$

III. Joint vs. Marginal MAP Estimation

The energy function in (5) is quadratic in **z**. By a rearrangement of variables, we may form the posterior distribution as the product of a function dependent only on **x** and a Gaussian distribution in **z** with mean,

$$\mathbf{m}_z(\mathbf{x}) = \mathbf{C}_z\mathbf{X}\mathbf{G}^T(\mathbf{G}\mathbf{X}\mathbf{C}_z\mathbf{X}\mathbf{G}^T + \mathbf{C}_n)^{-1}\mathbf{b} \quad (6)$$

and covariance,

$$\mathbf{Q}_z(\mathbf{x}) = \mathbf{X}\mathbf{G}^T\mathbf{C}_n^{-1}\mathbf{G}\mathbf{X} + \mathbf{C}_z^{-1}. \quad (7)$$

In joint MAP estimation, we find the $\mathbf{x}^*$ and $\mathbf{z}^*$ which minimize the energy function in (5). We recognize that the mean of a jointly Gaussian random vector corresponds to the maximizer of the distribution, and substitute $\mathbf{z}^*(\mathbf{x}) = \mathbf{m}_z(\mathbf{x})$ into the energy function in (5) to find a new energy function $\tilde{U}(\mathbf{x}|\mathbf{b})$. We can therefore first find the jointly optimal indicator process by minimizing $\tilde{U}(\mathbf{x}|\mathbf{b})$, then substitute this result into (6) to obtain the optimal amplitude process.

In marginal MAP estimation, we marginalize out the amplitude process from (3) by integrating over all possible **z**. The integral over all possible realizations of a Gaussian random process is the partition function $(2\pi)^{N/2}\det(\mathbf{Q}_z(\mathbf{x}))^{1/2}$. Using this property, we can find the marginalized posterior $p(\mathbf{x}|\mathbf{b})$ and find the marginalized MAP solution by minimizing the resulting energy function $U(\mathbf{x}|\mathbf{b})$. Note that this gives us no indication of the optimal $\mathbf{z}^*$, only a binary indicator of active sites. We can of course solve for the time series after computing the marginalized MAP estimate of activation sites.

To minimize $U(\mathbf{x}|\mathbf{b})$ or $\tilde{U}(\mathbf{x}|\mathbf{b})$ over all **x**, we use a continuation method based on mean field annealing (MFA)[3]. We visit each pixel in turn with the following update strategy,

$$x_i^{(n+1)} = E_T\{x_i | x_j^{(n)} \quad \forall\ j \neq i\} \quad (8)$$

where the conditional expectation is computed with respect to the modified probability,

$$p_T(\mathbf{x}|\mathbf{b}) = \frac{1}{Z_T}\exp\{-\frac{1}{T}U(\mathbf{x}|\mathbf{b})\}. \quad (9)$$

The temperature T is slowly reduced as the iterations proceed. As $T \to 0$ the iteration will converge to a binary solution [3] which is a local minimum of $U(\mathbf{x}|\mathbf{b})$ or $\tilde{U}(\mathbf{x}|\mathbf{b})$ depending on which MAP estimation method is used.

IV. Phantom Experiments

We applied the methods previously mentioned to experimental phantom data collected with a Neuromag-122 system [4] using the 26 dipole phantom supplied by the manufacturer. The Neuromag-122 employs 61 dual-channel planar first-order gradiometer units in a helmet-shaped configuration at a radius of 10-11 cm, for a total of 122 individual sensor measurements. The phantom consists of two half circles with a 7 cm radius in the x-z plane and y-z plane, with dipoles in fixed positions in these planes oriented tangential to the outer edge. The image grid consisted of 768 locations spaced 4 mm apart on these two half circles (See Fig. 1).

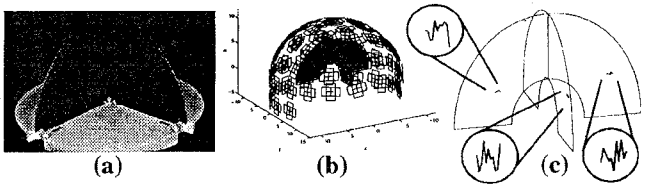

Fig. 1. (a) The phantom (b) Reconstruction region surrounded by the Neuromag-122 sensors (c) True image showing the time series of 3 active dipoles.

The phantom data was scaled to reflect a reasonable evoked field response. We then added data collected in the same system from a passive human subject (100 averages, eyes closed, no external stimulus present). This background was added to the phantom data to obtain a SNR of 8 dB. The results of one representative experiment are shown in Fig. 2.

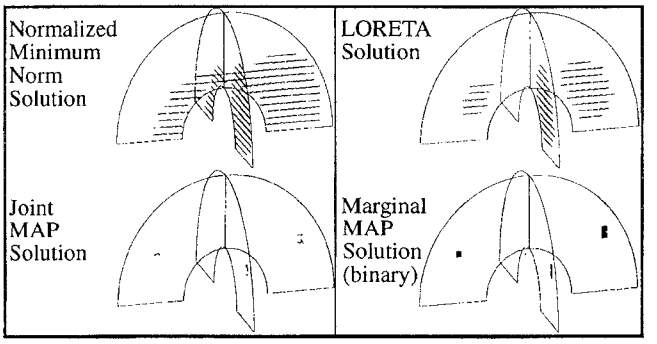

Fig. 2. Simulation results for the two minimum norm and the two MAP techniques (Noise added to make SNR 8dB).

V. Conclusions

All methods produced solutions which fitted the data well. In this sense, they are all physically (if not physiologically) plausible. Clearly, in order to select between these feasible solutions, we must have additional information concerning the expected nature of the source. Our Bayesian approaches specifically introduce sparse and focal information which results in generally superior results for sources that exhibit these characteristics.

VI. References

[1] B. Jeffs, R.M. Leahy, and M. Singh, "An evaluation of methods for neuromagnetic image reconstruction," *IEEE Trans on Bio Eng*, vol 34, pp 713-723, 1987.

[2] R.D. Pascual-Marqui *et. al.*, "Low resolution electromagnetic tomography: A new method for localizing electrical activity in the brain," *Int Journ of Psyc*,vol 18, pp 49-65, 1994.

[3] F. Bilbro *et. al.*, "Optimization by Mean Field Annealing," in: Touretzky D.S., *Advances in Neural Information Processing Systems*, Morgan-Kauffman, pp 91-98, 1989.

[4] M. Hämäläinen *et al.*, "Magnetoencephalography - theory, instrumentation, and applications to noninvasive studies of the working human brain," *Rev Mod Phys*, vol 65, no 2, pp 413-497, 1993.